Coherent control of optical injection of spin and currents in topological insulators

Rodrigo A. Muniz and J. E. Sipe
Department of Physics and Institute for Optical Sciences, University of Toronto, Toronto, Ontario, Canada, M5S 1A7
(Received 8 January 2014; revised manuscript received 29 March 2014; published 15 May 2014)

Topological insulators have surface states with a remarkable helical spin structure, with promising prospects for applications in spintronics. Strategies for generating spin-polarized currents, such as the use of magnetic contacts and photoinjection, have been the focus of extensive research. While several optical methods for injecting currents have been explored, they have all focused on one-photon absorption. Here we consider the use of both a fundamental optical field and its second harmonic, which allows the injection of spin-polarized carriers and current by a nonlinear process involving quantum interference between one- and two-photon absorption. General expressions are derived for the injection rates in a generic two-band system, including those for one- and two-photon absorption processes as well as their interference. Results are given for carrier, spin density, and current injection rates on the surface of topological insulators, for both linearly and circularly polarized light. We identify the conditions that would be necessary for experimentally verifying these predictions.

DOI: 10.1103/PhysRevB.89.205113 PACS number(s): 73.20.−r, 72.25.−b, 42.65.−k, 78.20.−e

I. INTRODUCTION

Three-dimensional topological insulators are fascinating materials, with a band gap in the bulk and protected midgap states at their surfaces [1,2]. The surface electronic bands are described by a single Dirac cone with a helical spin structure, which is the equivalent of a dominant Rashba spin-orbit coupling term in the Hamiltonian. This property leads to a number of interesting features, including nonmagnetic scattering, the magnetoelectric effect [3,4], and the formation of Majorana fermions in the proximity of superconductors [5]. Due to the effective spin-orbit coupling, the spin and current of the surface states are closely related [6], providing an exciting opportunity for technological applications using spin-polarized currents. There have already been several studies using the proximity of a magnetic metal for injecting spin polarization and current [7–10].

Another fruitful approach for manipulating currents in materials involves optical excitation. The optical properties of topological insulator surface states are very interesting themselves, with features such as the injected current depending explicitly on the Berry phase [11,12]. The injection of spin and current by one-photon absorption processes has been studied in different circumstances [12–14]. In order to break the rotational symmetry stemming from the Dirac cone—a necessary step for generating a current—the use of an in-plane magnetic field, the application of strain, and an oblique angle of incidence have all been considered. Corrections due to snowflake warping have been included; even a surprisingly relevant contribution from the Zeeman coupling of the light field has been identified [15]. Nonlinear effects due to the second harmonic have also been considered [16–19], especially in the treatment of pulses. However, the focus of even these studies has been on one-photon absorption processes.

One of the most interesting techniques for optical injection is coherent control, an example of which involves tuning the interference of one- and two-photon absorption processes to achieve a target response. This has been employed for injecting carriers, spin polarization, currents, and spin currents in semiconductors [20,21] and currents in graphene [22–24]. It has even been proposed that it could be used to inject a macroscopic Berry curvature in semiconductor quantum wells [25]. Here we present predictions of the optical injection of carrier density, spin polarization, charge current, and spin current at the surface of a topological insulator. In order to identify the fundamental properties of coherent control in topological insulators, we use a Hamiltonian with a perfectly symmetric Dirac cone, and we restrict the analysis to light at normal incidence. This also helps to contrast the results of coherent control with those obtained by other means. We keep a σ_z mass term in the Hamiltonian in order to analyze the dependence on the Berry phase, which has interesting effects on the injection rates.

In Sec. II we present the method used for the calculation of optical injection rates for an arbitrary quantity using Fermi's golden rule, considering one- and two-photon absorption processes as well as their interference. In Sec. III we provide general expressions for the injection rates of a generic two-band system, especially for carrier-density, spin-density, charge-current, and spin-current operators. Since two-band models can be used, as a first approximation, to compute optical properties of a large number of materials, the expressions derived there should be of use even beyond their application to topological insulators. In Sec. IV we apply the results of Sec. III to topological insulators. In Sec. V we present the results for linearly and circularly polarized light, referring to Appendixes A and B for details. In Sec. VI we end with a discussion of interesting features in our results and the possibilities for their experimental verification, including estimates for the expected experimental results. Since the experimental techniques required to confirm our results are well established, we can expect that such experiments will help advance the understanding and applications of topological insulators.

II. RESPONSE TO LIGHT FIELDS

There are several methods for computing the response of a system to external perturbations; one of the simplest and most standard methods is Fermi's golden rule. It is especially suitable for coherent control calculations because it makes

evident all the contributions stemming from one- and two-photon processes and their interference. This is a feature not shared by the Kubo formalism, for instance.

The calculation for the injection rates using Fermi's golden rule has been already well explained in previous studies [20]. However, it has been typically assumed that the fundamental photon energy is below the band gap, as is the case for most studies of semiconductors. Since we deal with systems that are gapless, there will be an additional interference term [26]. And in order to make the notation clear we present the main steps of the full calculation in the Supplemental Material [27]. Below we only show the main results.

We consider two incident light fields corresponding to the vector potential $\boldsymbol{A}(t) = \sum_{\omega_\alpha} \boldsymbol{A}(\omega_\alpha)\, e^{-i(\omega_\alpha + i\epsilon)t}$, with $\omega_\alpha = \pm\omega, \pm 2\omega$, and $\epsilon \to 0^+$ describes the turning on of the field from $t = -\infty$. The associated electric field is given by $\boldsymbol{E}(t) = -c^{-1}\partial_t \boldsymbol{A}(t)$. We then compute the injection rate for the density $\langle M \rangle$ of a quantity associated with a single-particle operator $\mathcal{M} = \sum_{\boldsymbol{k}} a^\dagger_{\alpha,\boldsymbol{k}} M_{\alpha\beta,\boldsymbol{k}} a_{\beta,\boldsymbol{k}}$; here α and β are band indices. It can be decomposed into contributions from one- and two-photon absorption processes with an additional interference term $\langle \dot{M} \rangle = \langle \dot{M}_1 \rangle + \langle \dot{M}_2 \rangle + \langle \dot{M}_i \rangle$, where

$$\begin{aligned}
\langle \dot{M}_1 \rangle &= \sum_{n=1,2} \Lambda_1^{bc}(n\omega) E^b(-n\omega) E^c(n\omega), \\
\langle \dot{M}_2 \rangle &= \Lambda_2^{bcde}(\omega) E^b(-\omega) E^c(-\omega) E^d(\omega) E^e(\omega), \\
\langle \dot{M}_i \rangle &= \sum_{n=1,2} \Lambda_{i(n)}^{bcd}(\omega) E^b(-\omega) E^c(-\omega) E^d(2\omega) + \text{c.c.},
\end{aligned} \tag{1}$$

with

$$\begin{aligned}
\Lambda_1^{bc}(n\omega) &= \frac{\pi}{L^D} \sum_{cv,c'v',\boldsymbol{k}} (M_{c'c,\boldsymbol{k}}\delta_{v'v} - M_{v'v,\boldsymbol{k}}\delta_{c'c}) \Gamma^{bc}_{1,c'v',cv}(\boldsymbol{k},\omega)[\delta(n\omega - \omega_{cv,\boldsymbol{k}}) + \delta(n\omega - \omega_{c'v',\boldsymbol{k}})], \\
\Lambda_2^{bcde}(\omega) &= \frac{\pi}{L^D} \sum_{cv,c'v',\boldsymbol{k}} (M_{c'c,\boldsymbol{k}}\delta_{v'v} - M_{v'v,\boldsymbol{k}}\delta_{c'c}) \Gamma^{bcde}_{2,c'v',cv}(\boldsymbol{k},\omega)[\delta(2\omega - \omega_{cv,\boldsymbol{k}}) + \delta(2\omega - \omega_{c'v',\boldsymbol{k}})], \\
\Lambda_{i(n)}^{bcd}(\omega) &= \frac{\pi}{L^D} \sum_{cv,c'v',\boldsymbol{k}} (M_{c'c,\boldsymbol{k}}\delta_{v'v} - M_{v'v,\boldsymbol{k}}\delta_{c'c}) \Gamma^{bcd}_{i(n),c'v',cv}(\boldsymbol{k},\omega)[\delta(n\omega - \omega_{cv,\boldsymbol{k}}) + \delta(n\omega - \omega_{c'v',\boldsymbol{k}})],
\end{aligned} \tag{2}$$

and

$$\begin{aligned}
\Gamma^{bc}_{1,c'v',cv}(\boldsymbol{k},\omega) &= \frac{e^2}{\hbar^2\omega^2} v^b_{v'c'} v^c_{cv}, \\
\Gamma^{bcde}_{2,c'v',cv}(\boldsymbol{k},\omega) &= \mathcal{W}^{bc}_{c'v',\boldsymbol{k}}(\omega,\omega)^* \mathcal{W}^{de}_{cv,\boldsymbol{k}}(\omega,\omega), \\
\Gamma^{bcd}_{i(1),c'v',cv}(\boldsymbol{k},\omega) &= \frac{ie}{\hbar\omega} v^b_{v'c'} \mathcal{W}^{cd}_{cv,\boldsymbol{k}}(2\omega,-\omega), \\
\Gamma^{bcd}_{i(2),c'v',cv}(\boldsymbol{k},\omega) &= \frac{ie}{2\hbar\omega} \mathcal{W}^{bc}_{cv,\boldsymbol{k}}(\omega,\omega)^* v^d_{c'v'},
\end{aligned} \tag{3}$$

where

$$\begin{aligned}
\Omega^{bc}_{cv,\boldsymbol{k}}(\omega_\alpha) &= \frac{-e^2}{\hbar^2\omega^2} \sum_n \frac{v^b_{cn} v^c_{nv}}{\omega_\alpha - \omega_{nv}}, \\
\mathcal{W}^{bc}_{cv,\boldsymbol{k}}(\omega_\alpha,\omega_\beta) &= \Omega^{bc}_{cv,\boldsymbol{k}}(\omega_\alpha) + \Omega^{cb}_{cv,\boldsymbol{k}}(\omega_\beta).
\end{aligned} \tag{4}$$

In the above equations, $\boldsymbol{v}$ is the velocity operator, the indices v and c correspond respectively to valence and conduction bands, $\hbar\omega_n$ is the energy of electrons at band n, and $\omega_{cv} = \omega_c - \omega_v$; L is the unidimensional normalization length, and D is the number of spatial dimensions of the system.

The $\Lambda_1^{bc}(\omega)$ and $\Lambda_{i(1)}^{bcd}(\omega)$ terms have usually been ignored in the literature, since they vanish for systems with a gap where the first harmonic falls below the band gap. The two interference processes are shown in Fig. 1. The quantities for which the injection rates will be computed are the densities associated with the carriers $\langle n \rangle$, spin $\langle \boldsymbol{S} \rangle$, charge current $\langle \boldsymbol{J}_c \rangle$, and spin current $\langle \boldsymbol{J}_S \rangle$. We denote the response coefficients associated with the quantities $\langle \dot{n} \rangle$, $\langle \dot{\boldsymbol{S}} \rangle$, $\langle \dot{\boldsymbol{J}}_c \rangle$, and $\langle \dot{\boldsymbol{J}}_S \rangle$, respectively, by ξ, ζ, η, and μ.

III. TWO-BAND SYSTEMS

Any Hermitian 2×2 matrix can be written as a linear combination of Pauli matrices σ and the identity σ_0. So a generic Hamiltonian for two bands is $\mathcal{H} = \sum_{\boldsymbol{k}} a^\dagger_{\alpha,\boldsymbol{k}} H_{\alpha\beta,\boldsymbol{k}} a_{\beta,\boldsymbol{k}}$, where $\alpha, \beta = 1,2$ are band indices, and

$$H_{\boldsymbol{k}} = \hbar\varpi_{\boldsymbol{k}}\sigma_0 + \hbar\boldsymbol{d}_{\boldsymbol{k}} \cdot \boldsymbol{\sigma} \tag{5}$$

denotes the Hamiltonian at each lattice momentum $\boldsymbol{k}$. The eigenenergies are $E_{\boldsymbol{k}\pm} = \hbar(\varpi_{\boldsymbol{k}} \pm d_{\boldsymbol{k}})$ where $d_{\boldsymbol{k}} = |\boldsymbol{d}_{\boldsymbol{k}}|$, with $(+) = c$ and $(-) = v$ representing the conduction and valence bands, respectively, so $\omega_{cv,\boldsymbol{k}} = 2d_{\boldsymbol{k}}$. The eigenstates satisfy $\hat{\boldsymbol{d}}_{\boldsymbol{k}} \cdot \boldsymbol{\sigma}\, \psi_{\boldsymbol{k}\pm} = \pm\psi_{\boldsymbol{k}\pm}$, so when $\hat{\boldsymbol{d}}_{\boldsymbol{k}} \cdot \boldsymbol{\sigma}$ is diagonalized it is

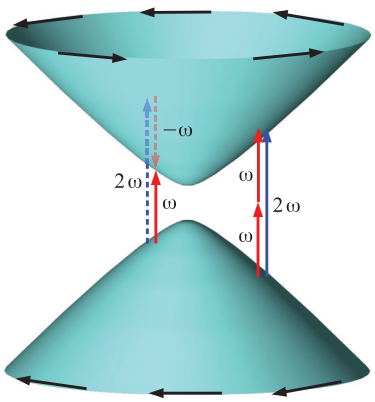

FIG. 1. (Color online) One- and two-photon interference processes illustrated on the helical Dirac cone. The one on the left has energy $\hbar\omega$ and corresponds to $(i)1$, while the one on the right has energy $2\hbar\omega$ and corresponds to $(i)2$.

represented by σ_z, and there is a unitary matrix $U_{\boldsymbol{k}}$ that performs the change of basis, $\hat{\boldsymbol{d}}_{\boldsymbol{k}} \cdot \boldsymbol{\sigma} = U_{\boldsymbol{k}} \sigma_z U_{\boldsymbol{k}}^\dagger$. Because SU(2) and SO(3) have the same algebra, we can write $U_{\boldsymbol{k}} \sigma_z U_{\boldsymbol{k}}^\dagger = (\mathcal{R}_{\boldsymbol{k}} \hat{\boldsymbol{z}}) \cdot \boldsymbol{\sigma}$, where $\mathcal{R}_{\boldsymbol{k}}$ represents a rotation around the axis $\hat{\boldsymbol{n}}_{\boldsymbol{k}}$ by an angle $\phi_{\boldsymbol{k}}$, so $U_{\boldsymbol{k}} = \exp(-i \frac{\phi_{\boldsymbol{k}}}{2} \hat{\boldsymbol{n}}_{\boldsymbol{k}} \cdot \boldsymbol{\sigma})$; we put $\hat{\boldsymbol{n}}_{\boldsymbol{k}} = \hat{\boldsymbol{z}} \times \hat{\boldsymbol{d}}_{\boldsymbol{k}} / |\hat{\boldsymbol{z}} \times \hat{\boldsymbol{d}}_{\boldsymbol{k}}|$ and $\cos \phi_{\boldsymbol{k}} = \hat{\boldsymbol{z}} \cdot \hat{\boldsymbol{d}}_{\boldsymbol{k}}$. The triad $\Xi = \{\hat{\boldsymbol{n}}_{\boldsymbol{k}}, \hat{\boldsymbol{d}}_{\boldsymbol{k}}, \hat{\boldsymbol{n}}_{\boldsymbol{k}} \times \hat{\boldsymbol{d}}_{\boldsymbol{k}}\}$ forms an orthonormal basis, so an arbitrary operator $\hat{\boldsymbol{w}} \cdot \boldsymbol{\sigma}$ can be easily written in the basis of eigenvectors $U_{\boldsymbol{k}}^\dagger (\hat{\boldsymbol{w}} \cdot \boldsymbol{\sigma}) U_{\boldsymbol{k}}$ by decomposing $\hat{\boldsymbol{w}}$ in the triad Ξ and performing the rotation $\mathcal{R}_{\boldsymbol{k}}$.

A. Operators

We keep track of the injected carriers by computing the density of electrons injected into the conduction band. The corresponding number operator has matrix elements $n_{cc} = 1$ and $n_{vv} = 0$. We suppose that the components of the spin operator are given by $S^a = \frac{\hbar}{2} \hat{\boldsymbol{a}} \cdot \boldsymbol{\sigma}$, and we decompose $\hat{\boldsymbol{a}} \cdot \boldsymbol{\sigma}$ according to Ξ, so

$$\begin{aligned} S^a_{cc} &= \frac{\hbar}{2} \hat{\boldsymbol{d}}_{\boldsymbol{k}} \cdot \hat{\boldsymbol{a}}, \\ S^a_{vv} &= -\frac{\hbar}{2} \hat{\boldsymbol{d}}_{\boldsymbol{k}} \cdot \hat{\boldsymbol{a}} \end{aligned} \tag{6}$$

are the matrix elements needed. Note that even though S^a_{cc} and S^a_{vv} are matrix elements of the spin operator in the basis of eigenstates, they are being expressed in terms of the parameters of the Hamiltonian in its nondiagonal form of Eq. (5).

The matrix associated with the velocity operator is [28]

$$v^a_{\boldsymbol{k}} = \frac{1}{\hbar} \partial_{k^a} H_{\boldsymbol{k}} = \partial_{k^a} \varpi_{\boldsymbol{k}} \sigma_0 + \partial_{k^a} \boldsymbol{d}_{\boldsymbol{k}} \cdot \boldsymbol{\sigma}, \tag{7}$$

and decomposing it according to Ξ gives the matrix elements

$$\begin{aligned} v^a_{cc} &= \partial_{k^a} \varpi_{\boldsymbol{k}} + \partial_{k^a} d_{\boldsymbol{k}}, \\ v^a_{vv} &= \partial_{k^a} \varpi_{\boldsymbol{k}} - \partial_{k^a} d_{\boldsymbol{k}}, \\ v^a_{cv} &= d_{\boldsymbol{k}} (\hat{\boldsymbol{n}}_{\boldsymbol{k}} + i \hat{\boldsymbol{n}}_{\boldsymbol{k}} \times \hat{\boldsymbol{d}}_{\boldsymbol{k}}) \cdot (\partial_{k^a} \hat{\boldsymbol{d}}_{\boldsymbol{k}}) \hat{\boldsymbol{n}}_{\boldsymbol{k}} \cdot (\hat{\boldsymbol{x}} - i \hat{\boldsymbol{y}}), \\ v^a_{vc} &= d_{\boldsymbol{k}} (\hat{\boldsymbol{n}}_{\boldsymbol{k}} - i \hat{\boldsymbol{n}}_{\boldsymbol{k}} \times \hat{\boldsymbol{d}}_{\boldsymbol{k}}) \cdot (\partial_{k^a} \hat{\boldsymbol{d}}_{\boldsymbol{k}}) \hat{\boldsymbol{n}}_{\boldsymbol{k}} \cdot (\hat{\boldsymbol{x}} + i \hat{\boldsymbol{y}}). \end{aligned} \tag{8}$$

It is also necessary to compute products of two velocity matrix elements,

$$v^a_{cv} v^b_{vc} = d^2_{\boldsymbol{k}} [\partial_{k^a} \hat{\boldsymbol{d}}_{\boldsymbol{k}} \cdot \partial_{k^b} \hat{\boldsymbol{d}}_{\boldsymbol{k}} + i \hat{\boldsymbol{d}}_{\boldsymbol{k}} \cdot (\partial_{k^a} \hat{\boldsymbol{d}}_{\boldsymbol{k}} \times \partial_{k^b} \hat{\boldsymbol{d}}_{\boldsymbol{k}})]. \tag{9}$$

The second term above is the Berry curvature; we can track the contributions to optical properties that depend on it. The charge current is expressed in terms of the velocity operator by $\boldsymbol{J}_c = e \boldsymbol{v}$.

We define the spin-current operator as $J^{ab}_{S,\boldsymbol{k}} = \frac{1}{2} (S^a v^b_{\boldsymbol{k}} + v^b_{\boldsymbol{k}} S^a)$, so for a system where $S^a = \frac{\hbar}{2} \hat{\boldsymbol{a}} \cdot \boldsymbol{\sigma}$ we have

$$\begin{aligned} J^{ab}_{S,cc} &= \hbar \frac{\hat{\boldsymbol{a}} \cdot \hat{\boldsymbol{d}}_{\boldsymbol{k}} (\partial_{k^b} d_{\boldsymbol{k}}) + d_{\boldsymbol{k}} \hat{\boldsymbol{a}} \cdot \partial_{k^b} \hat{\boldsymbol{d}}_{\boldsymbol{k}} + (\partial_{k^b} \varpi_{\boldsymbol{k}}) \hat{\boldsymbol{a}} \cdot \hat{\boldsymbol{d}}_{\boldsymbol{k}}}{2}, \\ J^{ab}_{S,vv} &= \hbar \frac{\hat{\boldsymbol{a}} \cdot \hat{\boldsymbol{d}}_{\boldsymbol{k}} (\partial_{k^b} d_{\boldsymbol{k}}) + d_{\boldsymbol{k}} \hat{\boldsymbol{a}} \cdot \partial_{k^b} \hat{\boldsymbol{d}}_{\boldsymbol{k}} - (\partial_{k^b} \varpi_{\boldsymbol{k}}) \hat{\boldsymbol{a}} \cdot \hat{\boldsymbol{d}}_{\boldsymbol{k}}}{2}, \end{aligned} \tag{10}$$

which completes the list of necessary matrix elements. Based on this, the coefficients used in Eqs. (2)–(4) are computed and shown explicitly in the Supplemental Material [29].

IV. TOPOLOGICAL INSULATORS

When the photon energy is smaller than the bulk band gap of a topological insulator, only the protected states localized on their surfaces will contribute to the optical absorption and injection.

The standard effective model describing the states on the surface of a topological insulator has a 2×2 Hamiltonian [30,31] given by

$$H_{\boldsymbol{k}} = \hbar (C_0 + D_0 k^2) \sigma_0 - \hbar A_0 (\hat{\boldsymbol{z}} \times \boldsymbol{k}) \cdot \boldsymbol{\sigma} + \hbar \Delta_m \sigma_z, \tag{11}$$

including terms up to the second order in $\boldsymbol{k}$. The $\Delta_m \sigma_z$ mass term is kept to keep track of how the Berry curvature affects the optical response; it would correspond to an external magnetic field along the $\hat{\boldsymbol{z}}$ direction, for instance. This Hamiltonian corresponds to Eq. (5) with $\varpi_{\boldsymbol{k}} = C_0 - Dk^2$ and $\boldsymbol{d}_{\boldsymbol{k}} = A_0 (\hat{\boldsymbol{z}} \times \boldsymbol{k}) + \Delta_m \hat{\boldsymbol{z}}$, so $\hat{\boldsymbol{n}}_{\boldsymbol{k}} = -\hat{\boldsymbol{k}}$ and

$$\begin{aligned} \partial_{k^b} d_{\boldsymbol{k}} &= \frac{A_0^2 k^b}{d_{\boldsymbol{k}}}, \\ \partial_{k^b} \hat{\boldsymbol{d}}_{\boldsymbol{k}} &= \frac{-A_0 (\hat{\boldsymbol{z}} \times \hat{\boldsymbol{b}})}{d_{\boldsymbol{k}}} - \frac{A_0^2 k^b \hat{\boldsymbol{d}}_{\boldsymbol{k}}}{d^2_{\boldsymbol{k}}}. \end{aligned} \tag{12}$$

This allows us to compute the optical injection coefficients. Since in the basis of Eq. (11) the spin operator is represented by $S^a = \frac{\hbar}{2} \hat{\boldsymbol{a}} \cdot \boldsymbol{\sigma}$, from Eqs. (6), (8), and (10) we can identify the matrix elements of the operators of interest:

$$\begin{aligned} S^a_{cc} - S^a_{vv} &= \hbar \hat{\boldsymbol{a}} \cdot \hat{\boldsymbol{d}}_{\boldsymbol{k}} = \frac{\hbar A_0 k^{z \times a} + \hbar \Delta_m \hat{\boldsymbol{z}} \cdot \hat{\boldsymbol{a}}}{d_{\boldsymbol{k}}}, \\ v^a_{cc} - v^a_{vv} &= 2 \partial_{k^a} d_{\boldsymbol{k}} = \frac{2 A_0^2 k^a}{d_{\boldsymbol{k}}}, \\ J^{ab}_{S,cc} - J^{ab}_{S,vv} &= \hbar (\partial_{k^b} \varepsilon_k) \hat{\boldsymbol{a}} \cdot \hat{\boldsymbol{d}}_{\boldsymbol{k}} = \frac{2 \hbar D_0 k^b [A_0 k^{z \times a} + \Delta_m \hat{\boldsymbol{z}} \cdot \hat{\boldsymbol{a}}]}{d_{\boldsymbol{k}}}. \end{aligned} \tag{13}$$

They satisfy the relations

$$\begin{aligned} S^z_{cc} - S^z_{vv} &= \frac{\hbar \Delta_m}{d_{\boldsymbol{k}}} = \frac{\hbar \Delta_m}{d_{\boldsymbol{k}}} (n_{cc} - n_{vv}), \\ \boldsymbol{v} &= -\frac{2 A_0 \hat{\boldsymbol{z}} \times \boldsymbol{S}}{\hbar}, \\ J^{zb}_{S,cc} - J^{zb}_{S,vv} &= \frac{2 \hbar D_0 k^b \Delta_m}{d_{\boldsymbol{k}}} = \frac{\hbar D_0 \Delta_m}{A_0^2} \left(v^b_{cc} - v^b_{vv} \right), \end{aligned} \tag{14}$$

where the second equation is the identity explored by Raghu *et al.* [6]; the first states that the $\hat{\boldsymbol{z}}$ component of the spin density S^z merely corresponds to the spin polarization of the injected carriers, and the third identifies the $\hat{\boldsymbol{z}}$ component of the spin current J^z_S as entirely due to the spin polarization of the charge current. Both spin density and current are nonzero only in the presence of the σ_z mass Δ_m. It should be noted that the spin current is typically not a conserved quantity, and indeed it is not conserved at the surface of topological insulators. Nevertheless, we still compute its optical injection rate because, depending on the experimental technique, the spin separation to which it leads might be detected (or tunneled to another material) before the spins relax [32,33].

The equations necessary for computing the optical injection coefficients are shown in the Supplemental Material [34]. The expressions for the various coefficients that follow from these

TABLE I. Values of the parameters used for the plots.

A_0 (m/s)	D_0 (m^2/s)	$\hbar\Delta_m$ (eV)	$\lvert E(\omega)\rvert$ (V/m)	$\lvert E(2\omega)\rvert$ (V/m)
5×10^5	7×10^{-4}	1.5×10^{-2}	1×10^4	72

expressions are the main results of this paper and are detailed in Appendix B.

V. RESULTS

For the system we are considering, one- and two-photon absorption processes inject scalar quantities while interference processes inject vectorial ones. We confirm within our model that carriers are injected by one- and two-photon absorption processes, but not from the interference between them. Conversely, charge current is injected solely from the interference processes and not from the one- and two-photon absorption processes. However, there are additional peculiarities for the spin density and spin current injection.

Due to relations (14), the in-plane spin density follows the charge current injection, stemming only from the interference processes; the out-of-plane spin density only has contributions from the one- and two-photon absorption processes. It simply corresponds to the spin polarization of the injected carriers, which is proportional to the σ_z mass term in the Hamiltonian.

A similar situation holds for the spin current. The spin current of the $\hat{z}$ component of spin follows the charge current and simply amounts to the net spin polarization of the carriers of the current; it is obtained from the interference terms. On the other hand, the in-plane spin current is a result of the Dirac cone with chiral spins; it does not require a net spin polarization generated by a σ_z mass term. It is obtained from one- and two-photon absorption and has no contribution from interference processes.

Below we present the injection rates for the quantities of interest, considering linear and circular polarizations. In Appendix A we show the general expressions for the optical injection coefficients, and in Appendix B we present the explicit form of the coefficients related to linear and circular polarizations of the incident light, which are referred to below.

The values of the parameters A_0, D_0, and $\Delta_m = \mu_B g B/(2\hbar)$ used for the plots or specific estimates are given in Table I; they correspond to the parameters of Bi_2Te_3 for an applied magnetic field around 10 T [30].

We consider field amplitudes of $E_\omega = 10^4$ V/m for the fundamental and $E_{2\omega} = 72$ V/m for the second harmonic, which are indicative of the largest field intensities allowed within the perturbative regime. These values depend on the expressions for the injected carrier density, so we explain how they are obtained in Sec. VI.

A. Linear polarizations

The one- and two-photon processes do not depend on the relative orientation of the fundamental $\boldsymbol{E}(\omega) = E_\omega e^{i\theta_1}\hat{\boldsymbol{e}}_\omega$ and second harmonic $\boldsymbol{E}(2\omega) = E_{2\omega}e^{i\theta_2}\hat{\boldsymbol{e}}_{2\omega}$ fields, where E_ω and $E_{2\omega}$ are real. Therefore, we show here the results for the injection coefficients Λ_1 and Λ_2, while the results for $\Lambda_{i(1)}$ and $\Lambda_{i(2)}$ are displayed for the special cases of parallel and perpendicular polarizations.

The carrier-density injection rate is given by

$$\begin{aligned}\langle \dot{n}_1\rangle &= \xi_1^{xx}(\omega)E_\omega^2 + \xi_1^{xx}(2\omega)E_{2\omega}^2,\\ \langle \dot{n}_2\rangle &= \xi_2^{xxxx}(\omega)E_\omega^4,\end{aligned} \tag{15}$$

and the $\hat{z}$ component of the spin-density injection rate is given by

$$\begin{aligned}\left\langle \dot{S}_1^z\right\rangle &= \frac{2\hbar\Delta_m}{\omega}\left[\xi_1^{xx}(\omega)\,E_\omega^2 + \frac{1}{2}\xi_1^{xx}(2\omega)\,E_{2\omega}^2\right],\\ \left\langle \dot{S}_2^z\right\rangle &= \frac{\hbar\Delta_m}{\omega}\xi_2^{xxxx}(\omega)\,E_\omega^4.\end{aligned} \tag{16}$$

This result simply corresponds to the net polarization of the injected carriers.

The charge-current injection rate vanishes; $\langle \dot{J}_1^a\rangle = \langle \dot{J}_2^a\rangle = 0$.

The spin-current injection rate is

$$\begin{aligned}\left\langle \dot{J}_{S,1}^{ab}\right\rangle &= \sum_{n=1,2}(\hat{z}\times\hat{\boldsymbol{e}}_{n\omega})\cdot\hat{\boldsymbol{a}}(\hat{\boldsymbol{e}}_{n\omega}\cdot\hat{\boldsymbol{b}})\mu_1^{yxxx}(n\omega)\,E_{n\omega}^2\\ &\quad+\sum_{n=1,2}\hat{\boldsymbol{e}}_{n\omega}\cdot\hat{\boldsymbol{a}}(\hat{z}\times\hat{\boldsymbol{e}}_{n\omega})\cdot\hat{\boldsymbol{b}}\mu_1^{xyxx}(n\omega)\,E_{n\omega}^2,\\ \left\langle \dot{J}_{S,2}^{ab}\right\rangle &= (\hat{z}\times\hat{\boldsymbol{e}}_{n\omega})\cdot\hat{\boldsymbol{a}}(\hat{\boldsymbol{e}}_{n\omega}\cdot\hat{\boldsymbol{b}})\mu_2^{yxxxxx}(\omega)\,E_\omega^4\\ &\quad+\hat{\boldsymbol{e}}_\omega\cdot\hat{\boldsymbol{a}}\,(\hat{z}\times\hat{\boldsymbol{e}}_\omega)\cdot\hat{\boldsymbol{b}}\mu_2^{xyxxxx}(\omega)\,E_\omega^4,\end{aligned} \tag{17}$$

where the first term in each equation gives a spin current independent of the applied field polarization and is due the helical spin structure.

1. Parallel orientations

Only the interference processes depend on the relative orientation of the $\boldsymbol{E}(\omega)$ and $\boldsymbol{E}(2\omega)$. Here the fields are $\boldsymbol{E}(\omega) = E_\omega e^{i\theta_1}\hat{\boldsymbol{e}}_\omega$ and $\boldsymbol{E}(2\omega) = E_{2\omega}e^{i\theta_2}\hat{\boldsymbol{e}}_\omega$. The relative phase parameter is $\Delta\theta = \theta_2 - 2\theta_1$.

The charge-current injection rate is given by

$$\langle \dot{\boldsymbol{J}}_i\rangle = -2\hat{\boldsymbol{e}}_\omega \mathrm{Im}\left[\eta_{i(1)}^{xxxx}(\omega) + \eta_{i(2)}^{xxxx}(\omega)\right]\sin(\Delta\theta)\,E_\omega^2 E_{2\omega}. \tag{18}$$

Due to Eq. (14), the in-plane spin density and the spin $\hat{z}$ current injection rates are given in terms of $\langle \dot{\boldsymbol{J}}_i(\omega)\rangle$ by

$$\begin{aligned}\langle \dot{\boldsymbol{S}}_i\rangle &= \frac{\hbar}{2A_0 e}\hat{z}\times\langle \dot{\boldsymbol{J}}_i\rangle,\\ \left\langle \dot{\boldsymbol{J}}_{S,i}^z\right\rangle &= \frac{\hbar D_0\Delta_m}{A_0^2 e}\langle \dot{\boldsymbol{J}}_i\rangle,\end{aligned} \tag{19}$$

and the spin current merely corresponds to the magnetization of the carriers of the charge current.

The direction of the polarization vector provides control of the angle of the injected vectorial quantities, while the relative phase parameter of the light beams can control only their magnitude and orientation.

2. Perpendicular orientations

Here we have $\boldsymbol{E}(\omega) = E_\omega e^{i\theta_1}\hat{\boldsymbol{e}}_\omega$ and $\boldsymbol{E}(2\omega) = E_{2\omega}e^{i\theta_2}\hat{\boldsymbol{e}}_{2\omega}$ with $\hat{\boldsymbol{e}}_{2\omega} = \hat{\boldsymbol{z}} \times \hat{\boldsymbol{e}}_\omega$. The relative phase parameter is again $\Delta\theta = \theta_2 - 2\theta_1$.

The charge-current injection rate is given by

$$\begin{aligned}\left\langle j_i^a \right\rangle = &-2\hat{\boldsymbol{e}}_{2\omega}\cdot\hat{\boldsymbol{a}}\,\mathrm{Im}\left[\eta_{i(1)}^{yxxy}(\omega) + \eta_{i(2)}^{yxxy}(\omega)\right]\sin(\Delta\theta)\,E_\omega^2 E_{2\omega} \\ &+ 2\hat{\boldsymbol{e}}_\omega\cdot\hat{\boldsymbol{a}}\,\mathrm{Re}\left[\eta_{i(1)}^{xxxy}(\omega) + \eta_{i(2)}^{xxxy}(\omega)\right] \\ &\times \cos(\Delta\theta)\,E_\omega^2 E_{2\omega}, \end{aligned} \tag{20}$$

and the spin density and current follow Eq. (19). From Eqs. (B6) and (B7) in Appendix B we can identify two different contributions to the injection: one that is related to the Berry curvature and thus depends on Δ_m, and another that is independent of Δ_m. Again the direction of the polarization vector provides control of the angle of the injected vectorial quantities. The relative phase can still control their magnitude and orientation, but it can also switch between the two regimes: the first where the photoinjection stems from the Berry curvature, and the second where it does not.

B. Circular polarizations

For circular polarizations $\boldsymbol{E}(\omega) = E_\omega e^{i\theta_1}\hat{\boldsymbol{p}}_{\tau_1}$ and $\boldsymbol{E}(2\omega) = E_{2\omega}e^{i\theta_2}\hat{\boldsymbol{p}}_{\tau_2}$, where $\tau_1,\tau_2 = \pm 1$ and $\hat{\boldsymbol{p}}_\pm = (\hat{\boldsymbol{x}} \pm i\hat{\boldsymbol{y}})/\sqrt{2}$, so $\hat{\boldsymbol{p}}_\tau \cdot \hat{\boldsymbol{p}}_\tau = 0$ and $\hat{\boldsymbol{p}}_+ \cdot \hat{\boldsymbol{p}}_- = 1$ as well as $\hat{\boldsymbol{p}}_- \times \hat{\boldsymbol{p}}_+ = i\hat{\boldsymbol{z}}$. The relative phase parameter is still $\Delta\theta = \theta_2 - 2\theta_1$. Again the one- and two-photon processes do not depend on the relative helicity of the $\boldsymbol{E}(\omega)$ and $\boldsymbol{E}(2\omega)$ fields and are presented first.

The carrier-density injection rate is now given by

$$\begin{aligned}\langle \dot{n}_1 \rangle &= \xi_1^{-+}(\omega)\,E_\omega^2 + \xi_1^{-+}(2\omega)\,E_{2\omega}^2, \\ \langle \dot{n}_2 \rangle &= \xi_2^{--++}(\omega)\,E_\omega^4. \end{aligned} \tag{21}$$

The spin-density injection is still given by Eq. (16), and for the spin current we have

$$\begin{aligned}\left\langle j_{S,1}^{ab} \right\rangle &= 2i(\hat{\boldsymbol{a}}\times\hat{\boldsymbol{b}})\cdot\hat{\boldsymbol{z}}\sum_{n=1,2}\mu_1^{-+-+}(n\omega)\,E_{n\omega}^2, \\ \left\langle j_{S,2}^{ab} \right\rangle &= 2i(\hat{\boldsymbol{a}}\times\hat{\boldsymbol{b}})\cdot\hat{\boldsymbol{z}}\mu_2^{-+--++}(\omega)\,E_\omega^4. \end{aligned} \tag{22}$$

Circularly polarized light does not break rotational symmetry; therefore, the second term of Eq. (17) is not present.

1. Equal helicities

The interference processes depend on the relative helicity of the two fields. We first consider the fields with the same helicity, $\boldsymbol{E}(\omega) = E_\omega e^{i\theta_1}\hat{\boldsymbol{p}}_\tau$ and $\boldsymbol{E}(2\omega) = E_{2\omega}e^{i\theta_2}\hat{\boldsymbol{p}}_\tau$.

The charge-current injection rate is given by

$$\begin{aligned}\left\langle j_i^a \right\rangle = &\,2[a^y\cos(\Delta\theta) + a^x\sin(\Delta\theta)] \\ &\times i[\eta_{i(1)}^{+--+}(\omega) + \eta_{i(2)}^{+--+}(\omega)]E_\omega^2 E_{2\omega}. \end{aligned} \tag{23}$$

The spin density and current follow Eq. (19).

The relative phase displacement between the two light beams can now control the direction of the injected quantities.

Especially for frequencies near the gap, the injection rates for different helicities τ depend strongly on the chirality of the electronic states, identified by $\Delta_m/|\Delta_m|$. The helicity of the incident light has no effect for vanishing Δ_m.

2. Opposite helicities

Here we have $\boldsymbol{E}(\omega) = E_\omega e^{i\theta_1}\hat{\boldsymbol{p}}_\tau$ and $\boldsymbol{E}(2\omega) = E_{2\omega}e^{i\theta_2}\hat{\boldsymbol{p}}_{-\tau}$. The injection rates from interference all vanish for the four operators of interest.

VI. DISCUSSION

In order to determine the validity of our calculations for the optical injection rates, we have to consider the fraction of the injected carrier population relative to the total number of states in the range of energies covered by the laser pulse. The duration of the pulse, $\mathcal{T}$, sets the minimum frequency broadening of the laser pulse $\Delta\omega = \frac{2\pi}{\mathcal{T}}$, which in turn—via the dispersion relation, which we assume is $E_{\boldsymbol{k}} = \hbar A_0 k$ here for simplicity—determines the area of the Brillouin zone that can be populated by carriers: $a = 2\pi k\Delta k$, where $k = \frac{\omega}{A_0}$ and $\Delta k = \frac{\Delta\omega}{A_0}$. The number of states available in this area of the Brillouin zone is a/a_1, where $a_1 = \frac{(2\pi)^2}{L^2}$ is the area occupied by one state. The maximum amplitudes of the laser fields are restricted by the condition that the number of injected carriers with additional energy $2\hbar\omega$ is at most 5% of the total number of carrier states in the allowed energy range:

$$\left(\xi_1^{xx}(2\omega)\,E_{2\omega}^2 + \xi_2^{xxxx}(\omega)\,E_\omega^4\right)\mathcal{T}L^2 < 0.05\frac{a}{a_1}. \tag{24}$$

We then estimate the amplitudes by imposing the additional condition $\xi_1^{xx}(2\omega)\,E_{2\omega}^2 = \xi_2^{xxxx}(\omega)\,E_\omega^4$, which gives optimal interference between the absorption processes [20]. Finally, the field amplitudes are limited by

$$(eE_{2\omega})^2 = \frac{4A_0^2(eE_\omega)^4}{\hbar^2\omega^4} < \frac{1.6\hbar^2\omega^2}{A_0^2\mathcal{T}^2}. \tag{25}$$

For pulses lasting 1 ns with a frequency of 30 meV, the field amplitudes found are $E_\omega = 1\times10^4$ V/m for the fundamental and $E_{2\omega} = 72$ V/m for the second harmonic, which correspond to laser intensities of 9.9 W/cm^2 and 0.65 mW/cm^2, respectively. We use these values for all $\hbar\omega$ in Figs. 2–4, although for $\hbar\omega <$ 30 meV smaller amplitudes would be required to guarantee Eq. (24) and could be found by using Eq. (25). Our estimates on the limit of perturbation theory neglect any relaxation of the injected carriers. Its presence will allow the use of

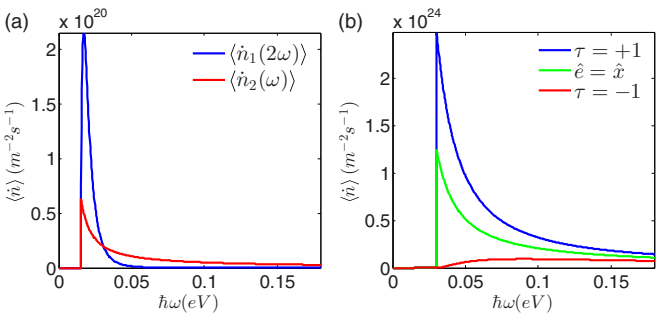

FIG. 2. (Color online) (a) Carrier-density injection rates from one- and two-photon absorption processes at total energy $2\hbar\omega$. (b) Carrier-density injection rates for linear ($\hat{\boldsymbol{e}}_\omega = \hat{\boldsymbol{x}}$) and circular ($\tau = \pm 1$) polarizations of the incident fields.

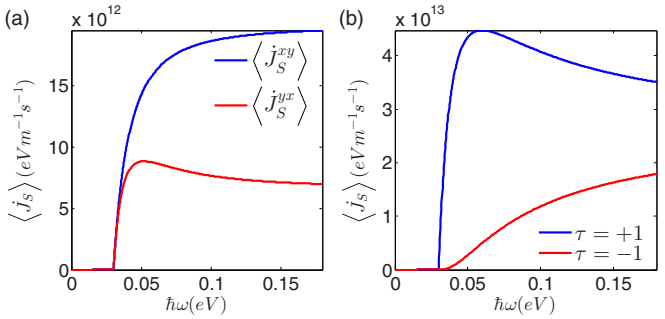

FIG. 3. (Color online) Planar spin current density injection rates for (a) linear polarizations along the $\hat{\boldsymbol{x}}$ direction and (b) circular polarizations.

higher-energy laser pulses to compensate for the relaxation, at least partially, without leaving the perturbative regime.

In the absence of the σ_z mass term, the carrier and charge-current injection rates are very similar to the ones found for graphene [23], except for the adjustments due to having only one Dirac cone and a smaller Fermi velocity. However, even in this case there is also injection of the transverse spin following the same form of the injected current, a signature characteristic of topological insulators. The magnitude of these injected quantities is also of the same order as the values for graphene, where the current injected by the processes discussed here has already been measured [22]. The carrier relaxation time is also longer for the surface of topological insulators than for graphene [35].

Another distinctive trait shared with graphene is the relatively low average velocity of the injected carriers when compared to semiconductors. This is due to the one-photon absorption at the fundamental frequency, forbidden in semiconductors because of the band gap. This gives rise to the extra interference process with total energy $\hbar\omega$, which usually partially cancels the injected current stemming from the interference process with total energy $2\hbar\omega$.

Several particular features are found in the presence of the Berry phase inducing the $\Delta_m\sigma_z$ term, especially for circular polarizations of the optical fields, when an interesting interplay between the helicity τ of the incident fields and the chirality $\Delta_m/|\Delta_m|$ of the Dirac cone can greatly suppress or enhance optical injection. In order to observe these features a combination of high magnetic field and low temperature is necessary, because the Zeeman coupling $\hbar\Delta_m = \mu_B g B/2$ needs to be above temperature $k_B T$. We estimate that 77 K and 6 T should be enough for Bi_2Te_3. For a pronounced effect, the photon energy should not be much larger than the Zeeman gap. Reasonable photon energies for the fundamental field would not be much larger than $\hbar\omega = 30$ meV, which can be achieved with quantum cascade lasers.

When lasers of similar intensity are considered, the predicted magnitude of the injected currents obtained from coherent control seem to be considerably larger than the values found by other approaches, such as applying an in-plane magnetic field or using oblique incidence. Therefore, it can play a crucial role in the quest for harnessing the exotic properties of topological insulators for spintronics applications.

ACKNOWLEDGMENTS

We thank Julien Rioux and Jin-Luo Cheng for helpful discussions. This work was supported by the Natural Sciences and Engineering Research Council of Canada (NSERC).

APPENDIX A: GENERAL EXPRESSIONS FOR THE OPTICAL INJECTION COEFFICIENTS

In order to express the optical injection coefficients, it is helpful to introduce the following quantities:

$$\begin{aligned}
\varphi^{ab} &= \int \frac{d\theta}{2\pi}\frac{k^a k^b}{k^2} = \frac{\hat{\boldsymbol{a}}\cdot\hat{\boldsymbol{b}}}{2},\\
\varphi^{abcd} &= \int \frac{d\theta}{2\pi}\frac{k^a k^b k^c k^d}{k^4}\\
&= \frac{\hat{\boldsymbol{a}}\cdot\hat{\boldsymbol{b}}(\hat{\boldsymbol{c}}\cdot\hat{\boldsymbol{d}}) + \hat{\boldsymbol{a}}\cdot\hat{\boldsymbol{c}}(\hat{\boldsymbol{b}}\cdot\hat{\boldsymbol{d}}) + \hat{\boldsymbol{a}}\cdot\hat{\boldsymbol{d}}(\hat{\boldsymbol{b}}\cdot\hat{\boldsymbol{c}})}{8},\\
\varphi^{abcdef} &= \int \frac{d\theta}{2\pi}\frac{k^a k^b k^c k^d k^e k^f}{k^6}\\
&= \sum_{\text{pairings}} \frac{\hat{\boldsymbol{a}}\cdot\hat{\boldsymbol{b}}(\hat{\boldsymbol{c}}\cdot\hat{\boldsymbol{d}})\hat{\boldsymbol{e}}\cdot\hat{\boldsymbol{f}}}{48}.
\end{aligned} \tag{A1}$$

Intermediate steps are shown in the Supplemental Material [36], which give the following results.

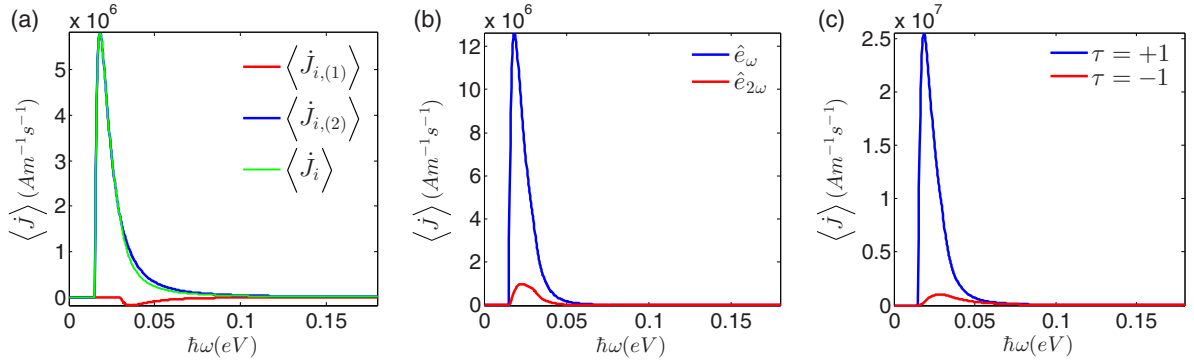

FIG. 4. (Color online) Current-density injection rates for (a) linear polarizations with parallel orientations, (b) linear polarizations with perpendicular orientations, showing the components of the current along the $\hat{\boldsymbol{e}}_\omega$ and $\hat{\boldsymbol{e}}_{2\omega}$ directions, and (c) circular polarizations.

1. One- and two-photon absorption

The carrier-density coefficients are

$$\xi_1^{bc}(\omega) = \frac{\Theta(\omega-2\Delta_m)e^2}{2\hbar^2\omega}\left[\frac{\hat{\boldsymbol{b}}\cdot\hat{\boldsymbol{c}}}{4}\left(1+\frac{4\Delta_m^2}{\omega^2}\right)-i\frac{\Delta_m\hat{\boldsymbol{z}}\cdot(\hat{\boldsymbol{b}}\times\hat{\boldsymbol{c}})}{\omega}\right],$$
$$\xi_2^{bcde}(\omega) = \frac{\Theta(\omega-\Delta_m)e^4A_0^2}{\hbar^4\omega^5}\left(1-\frac{\Delta_m^2}{\omega^2}\right)\left\{\left[\frac{(\hat{\boldsymbol{b}}\cdot\hat{\boldsymbol{d}})\hat{\boldsymbol{c}}\cdot\hat{\boldsymbol{e}}+(\hat{\boldsymbol{b}}\cdot\hat{\boldsymbol{e}})\hat{\boldsymbol{c}}\cdot\hat{\boldsymbol{d}}}{2}-2\varphi^{bcde}\left(1-\frac{\Delta_m^2}{\omega^2}\right)\right]\right.$$
$$\left.+i\frac{\Delta_m}{\omega}\left[\frac{\hat{\boldsymbol{c}}\cdot\hat{\boldsymbol{e}}(\hat{\boldsymbol{d}}\times\hat{\boldsymbol{b}})\cdot\hat{\boldsymbol{z}}+\hat{\boldsymbol{b}}\cdot\hat{\boldsymbol{e}}(\hat{\boldsymbol{d}}\times\hat{\boldsymbol{c}})\cdot\hat{\boldsymbol{z}}+\hat{\boldsymbol{c}}\cdot\hat{\boldsymbol{d}}(\hat{\boldsymbol{e}}\times\hat{\boldsymbol{b}})\cdot\hat{\boldsymbol{z}}+\hat{\boldsymbol{d}}\cdot\hat{\boldsymbol{b}}(\hat{\boldsymbol{e}}\times\hat{\boldsymbol{c}})\cdot\hat{\boldsymbol{z}}}{4}\right]\right\}. \tag{A2}$$

The charge-current coefficients vanish: $\eta_1^{abc}(\omega)=\eta_2^{abcde}(\omega)=0$.

The spin-density coefficients can be written in terms of the carrier-density ones as

$$\zeta_1^{abc}(\omega) = \frac{2\hbar\Delta_m(\hat{\boldsymbol{z}}\cdot\hat{\boldsymbol{a}})}{\omega}\xi_1^{bc}(\omega), \quad \zeta_2^{abcde}(\omega) = \frac{\hbar\Delta_m(\hat{\boldsymbol{z}}\cdot\hat{\boldsymbol{a}})}{\omega}\xi_2^{bcde}(\omega), \tag{A3}$$

which is a consequence of Eq. (14).

And the spin-current coefficients are

$$\mu_1^{abcd}(\omega) = \frac{\Theta(\omega-2\Delta_m)e^2D_0}{4A_0\hbar}\left(1-\frac{4\Delta_m^2}{\omega^2}\right)\left[\frac{(\hat{\boldsymbol{z}}\times\hat{\boldsymbol{a}})\cdot\hat{\boldsymbol{b}}(\hat{\boldsymbol{c}}\cdot\hat{\boldsymbol{d}})}{2}-\varphi^{(z\times a)bcd}\left(1-\frac{4\Delta_m^2}{\omega^2}\right)+i\frac{\Delta_m(\hat{\boldsymbol{z}}\times\hat{\boldsymbol{a}})\cdot\hat{\boldsymbol{b}}(\hat{\boldsymbol{d}}\times\hat{\boldsymbol{c}})\cdot\hat{\boldsymbol{z}}}{\omega}\right],$$
$$\mu_2^{abcdef}(\omega) = \frac{4\Theta(\omega-\Delta_m)e^4D_0A_0}{\hbar^3\omega^4}\left(1-\frac{\Delta_m^2}{\omega^2}\right)^2\left[\frac{\varphi^{(z\times a)bdf}\hat{\boldsymbol{c}}\cdot\hat{\boldsymbol{e}}+\varphi^{(z\times a)bcf}\hat{\boldsymbol{d}}\cdot\hat{\boldsymbol{e}}+\varphi^{(z\times a)bde}\hat{\boldsymbol{c}}\cdot\hat{\boldsymbol{f}}+\varphi^{(z\times a)bce}\hat{\boldsymbol{d}}\cdot\hat{\boldsymbol{f}}}{4}\right.$$
$$\left.-\varphi^{(z\times a)bcdef}\left(1-\frac{\Delta_m^2}{\omega^2}\right)\right]+i\frac{4\Theta(\omega-\Delta_m)e^4D_0A_0}{\hbar^3\omega^4}\frac{\Delta_m}{\omega}\left(1-\frac{\Delta_m^2}{\omega^2}\right)^2$$
$$\times\left[\frac{\varphi^{(z\times a)bdf}(\hat{\boldsymbol{e}}\times\hat{\boldsymbol{c}})\cdot\hat{\boldsymbol{z}}+\varphi^{(z\times a)bcf}(\hat{\boldsymbol{e}}\times\hat{\boldsymbol{d}})\cdot\hat{\boldsymbol{z}}+\varphi^{(z\times a)bde}(\hat{\boldsymbol{f}}\times\hat{\boldsymbol{c}})\cdot\hat{\boldsymbol{z}}+\varphi^{(z\times a)bce}(\hat{\boldsymbol{f}}\times\hat{\boldsymbol{d}})\cdot\hat{\boldsymbol{z}}}{4}\right], \tag{A4}$$

giving spin currents with only in-plane components of spin, which is independent of the $\Delta_m\sigma_z$ mass term.

2. Interference processes

The carrier-density coefficients vanish: $\xi_{i(n)}^{bcd}(\omega)=0$. The charge-current coefficients are

$$\eta_{i(1)}^{abcd}(\omega) = \frac{i\Theta(\omega-2\Delta_m)e^4A_0^2}{4\hbar^3\omega^3}\left(1-\frac{4\Delta_m^2}{\omega^2}\right)\left\{\left[\frac{(\hat{\boldsymbol{a}}\cdot\hat{\boldsymbol{d}})\hat{\boldsymbol{b}}\cdot\hat{\boldsymbol{c}}-2(\hat{\boldsymbol{a}}\cdot\hat{\boldsymbol{c}})\hat{\boldsymbol{b}}\cdot\hat{\boldsymbol{d}}}{2}+\varphi^{abcd}\left(1-\frac{4\Delta_m^2}{\omega^2}\right)\right]\right.$$
$$\left.+i\frac{2\Delta_m}{\omega}\left[\frac{\hat{\boldsymbol{a}}\cdot\hat{\boldsymbol{d}}(\hat{\boldsymbol{c}}\times\hat{\boldsymbol{b}})\cdot\hat{\boldsymbol{z}}-2\hat{\boldsymbol{a}}\cdot\hat{\boldsymbol{c}}(\hat{\boldsymbol{d}}\times\hat{\boldsymbol{b}})\cdot\hat{\boldsymbol{z}}}{2}\right]\right\},$$
$$\eta_{i(2)}^{abcd}(\omega) = \frac{i\Theta(\omega-\Delta_m)e^4A_0^2}{2\hbar^3\omega^3}\left(1-\frac{\Delta_m^2}{\omega^2}\right)\left\{\left[\frac{(\hat{\boldsymbol{a}}\cdot\hat{\boldsymbol{c}})\hat{\boldsymbol{b}}\cdot\hat{\boldsymbol{d}}+(\hat{\boldsymbol{a}}\cdot\hat{\boldsymbol{b}})\hat{\boldsymbol{c}}\cdot\hat{\boldsymbol{d}}}{2}-2\varphi^{abcd}\left(1-\frac{\Delta_m^2}{\omega^2}\right)\right]\right.$$
$$\left.+i\frac{\Delta_m}{\omega}\left[\frac{\hat{\boldsymbol{a}}\cdot\hat{\boldsymbol{c}}(\hat{\boldsymbol{d}}\times\hat{\boldsymbol{b}})\cdot\hat{\boldsymbol{z}}+\hat{\boldsymbol{a}}\cdot\hat{\boldsymbol{b}}(\hat{\boldsymbol{d}}\times\hat{\boldsymbol{c}})\cdot\hat{\boldsymbol{z}}}{2}\right]\right\}, \tag{A5}$$

due to Eq. (14), the spin-density coefficients can be written in terms of the ones for the charge current as

$$\zeta_{i(n)}^{abcd}(\omega) = \frac{\hbar}{2eA_0}\eta_{i(n)}^{(z\times a)bcd}(\omega), \tag{A6}$$

and the spin-current coefficients can also be written in terms of the ones for the charge current as

$$\mu_{i(n)}^{abcde}(\omega) = \frac{\hbar D_0\Delta_m\hat{\boldsymbol{z}}\cdot\hat{\boldsymbol{a}}}{eA_0^2}\eta_{i(n)}^{bcde}(\omega), \tag{A7}$$

which finishes the list of optical injection coefficients.

APPENDIX B: OPTICAL INJECTION COEFFICIENTS FOR LINEAR AND CIRCULAR POLARIZATIONS

The coefficients used in Sec. V for one- and two-photon absorption processes are

$$\xi_1^{xx}(\omega) = \frac{\Theta(\omega-2\Delta_m)e^2}{8\hbar^2\omega}\left(1+\frac{4\Delta_m^2}{\omega^2}\right),$$
$$\xi_2^{xxxx}(\omega) = \frac{\Theta(\omega-\Delta_m)e^4A_0^2}{4\hbar^4\omega^5}\left(1-\frac{\Delta_m^2}{\omega^2}\right)\left(1+\frac{3\Delta_m^2}{\omega^2}\right), \tag{B1}$$

and

$$\mu_1^{xyxx}(\omega) = \frac{\Theta(\omega-2\Delta_m)e^2D_0}{8\hbar A_0}\left(1-\frac{4\Delta_m^2}{\omega^2}\right)\left(\frac{3}{4}+\frac{\Delta_m^2}{\omega^2}\right),$$
$$\mu_1^{yxxx}(\omega) = -\frac{\Theta(\omega-2\Delta_m)e^2D_0}{8\hbar A_0}\left(1-\frac{4\Delta_m^2}{\omega^2}\right)\left(\frac{1}{4}+\frac{3\Delta_m^2}{\omega^2}\right),$$
$$\mu_2^{xyxxxx}(\omega) = \frac{\Theta(\omega-\Delta_m)e^4D_0A_0}{4\hbar^3\omega^4}\left(1-\frac{\Delta_m^2}{\omega^2}\right)^2\left(1+\frac{\Delta_m^2}{\omega^2}\right),$$
$$\mu_2^{yxxxxx}(\omega) = -\frac{\Theta(\omega-\Delta_m)e^4D_0A_0}{4\hbar^3\omega^4}\left(1-\frac{\Delta_m^2}{\omega^2}\right)^2\left(1+\frac{5\Delta_m^2}{\omega^2}\right), \tag{B2}$$

for linear polarization.

For circular polarization we have

$$\xi_1^{-\tau,+\tau}(\omega) = \frac{\Theta(\omega-2\Delta_m)e^2}{8\hbar^2\omega}\left(1+\tau\frac{2\Delta_m}{\omega^2}\right)^2,$$
$$\xi_2^{--++}(\omega) = \frac{\Theta(\omega-\Delta_m)e^4A_0^2}{2\hbar^4\omega^5}\left(1-\frac{\Delta_m^2}{\omega^2}\right)\left(1+\tau\frac{\Delta_m}{\omega}\right)^2, \tag{B3}$$

and

$$\mu_1^{-+-+}(\omega) = \frac{i\Theta(\omega-2\Delta_m)e^2D_0}{16\hbar A_0}\left(1-\frac{4\Delta_m^2}{\omega^2}\right)\left(1+\tau\frac{2\Delta_m}{\omega}\right)^2,$$
$$\mu_2^{-+--++}(\omega) = \frac{i\Theta(\omega-\Delta_m)e^4D_0A_0}{2\hbar^3\omega^4}\left(1-\frac{\Delta_m^2}{\omega^2}\right)^2\left(1+\tau\frac{\Delta_m}{\omega}\right)^2, \tag{B4}$$

also $\mu_1^{+--+}(\omega) = -\mu_1^{-+-+}(\omega)$ and $\mu_2^{-+--++}(\omega) = -\mu_2^{-+--++}(\omega)$.

The interference coefficients are

$$\eta_{i(1)}^{xxxx}(\omega) = \frac{-i\Theta(\omega-2\Delta_m)e^4A_0^2}{32\hbar^3\omega^3}\left(1-\frac{4\Delta_m^2}{\omega^2}\right)\left(1+\frac{12\Delta_m^2}{\omega^2}\right),$$
$$\eta_{i(2)}^{xxxx}(\omega) = \frac{i\Theta(\omega-\Delta_m)e^4A_0^2}{8\hbar^3\omega^3}\left(1-\frac{\Delta_m^2}{\omega^2}\right)\left(1+\frac{3\Delta_m^2}{\omega^2}\right), \tag{B5}$$

and

$$\eta_{i(1)}^{xxxy}(\omega) = -\frac{\Theta(\omega-2\Delta_m)e^4A_0^2}{2\hbar^3\omega^3}\left(1-\frac{4\Delta_m^2}{\omega^2}\right)\frac{\Delta_m}{\omega},$$
$$\eta_{i(2)}^{xxxy}(\omega) = \frac{\Theta(\omega-\Delta_m)e^4A_0^2}{2\hbar^3\omega^3}\left(1-\frac{\Delta_m^2}{\omega^2}\right)\frac{\Delta_m}{\omega}, \tag{B6}$$

also

$$\eta_{i(1)}^{yxxy}(\omega) = \frac{i\Theta(\omega-2\Delta_m)e^4A_0^2}{32\hbar^3\omega^3}\left(1-\frac{4\Delta_m^2}{\omega^2}\right)\left(5-\frac{4\Delta_m^2}{\omega^2}\right),$$
$$\eta_{i(2)}^{yxxy}(\omega) = \frac{-i\Theta(\omega-\Delta_m)e^4A_0^2}{8\hbar^3\omega^3}\left(1-\frac{\Delta_m^2}{\omega^2}\right)^2, \tag{B7}$$

and

$$\eta_{i(1)}^{+--+}(\omega) = \frac{i\Theta(\omega-2\Delta_m)e^4A_0^2}{4\hbar^3\omega^3}\left(1-\frac{4\Delta_m^2}{\omega^2}\right)\times\left[\frac{1}{4}-\left(1+\tau\frac{\Delta_m}{\omega}\right)^2\right],$$
$$\eta_{i(2)}^{+--+}(\omega) = \frac{i\Theta(\omega-\Delta_m)e^4A_0^2}{4\hbar^3\omega^3}\left(1-\frac{\Delta_m^2}{\omega^2}\right)\left(1+\tau\frac{\Delta_m}{\omega}\right)^2, \tag{B8}$$

from which the other injection coefficients are obtained.

[1] M. Z. Hasan and C. L. Kane, Rev. Mod. Phys. **82**, 3045 (2010).
[2] X.-L. Qi and S.-C. Zhang, Rev. Mod. Phys. **83**, 1057 (2011).
[3] X.-L. Qi, T. L. Hughes, and S.-C. Zhang, Phys. Rev. B **78**, 195424 (2008).
[4] A. M. Essin, J. E. Moore, and D. Vanderbilt, Phys. Rev. Lett. **102**, 146805 (2009).
[5] L. Fu and C. L. Kane, Phys. Rev. Lett. **100**, 096407 (2008).
[6] S. Raghu, S. B. Chung, X.-L. Qi, and S.-C. Zhang, Phys. Rev. Lett. **104**, 116401 (2010).
[7] C. Ojeda-Aristizabal, M. S. Fuhrer, N. P. Butch, J. Paglione, and I. Appelbaum, Appl. Phys. Lett. **101**, 023102 (2012).
[8] S. Modak, K. Sengupta, and D. Sen, Phys. Rev. B **86**, 205114 (2012).
[9] Y. G. Semenov, X. Li, and K. W. Kim, Phys. Rev. B **86**, 201401(R) (2012).
[10] F. Mahfouzi, N. Nagaosa, and B. K. Nikolić, Phys. Rev. Lett. **109**, 166602 (2012).
[11] W.-K. Tse and A. H. MacDonald, Phys. Rev. Lett. **105**, 057401 (2010).
[12] P. Hosur, Phys. Rev. B **83**, 035309 (2011).
[13] T. Misawa, T. Yokoyama, and S. Murakami, Phys. Rev. B **84**, 165407 (2011).
[14] J. W. McIver, D. Hsieh, H. Steinberg, P. Jarillo-Herrero, and N. Gedik, Nat. Nanotechnol. **7**, 96 (2012).
[15] A. Junck, G. Refael, and F. von Oppen, Phys. Rev. B **88**, 075144 (2013).
[16] D. Hsieh, J. W. McIver, D. H. Torchinsky, D. R. Gardner, Y. S. Lee, and N. Gedik, Phys. Rev. Lett. **106**, 057401 (2011).
[17] D. Hsieh, F. Mahmood, J. W. McIver, D. R. Gardner, Y. S. Lee, and N. Gedik, Phys. Rev. Lett. **107**, 077401 (2011).
[18] J. W. McIver, D. Hsieh, S. G. Drapcho, D. H. Torchinsky, D. R. Gardner, Y. S. Lee, and N. Gedik, Phys. Rev. B **86**, 035327 (2012).
[19] J. A. Sobota, S. Yang, J. G. Analytis, Y. L. Chen, I. R. Fisher, P. S. Kirchmann, and Z.-X. Shen, Phys. Rev. Lett. **108**, 117403 (2012).
[20] J. Rioux and J. E. Sipe, Physica E **45**, 1 (2012).
[21] K. M. Rao and J. E. Sipe, Phys. Rev. B **84**, 205313 (2011).
[22] D. Sun, C. Divin, J. Rioux, J. E. Sipe, C. Berger, W. A. de Heer, P. N. First, and T. B. Norris, Nano Lett. **10**, 1293 (2010).

[23] J. Rioux, G. Burkard, and J. E. Sipe, Phys. Rev. B **83**, 195406 (2011).
[24] K. M. Rao and J. E. Sipe, Phys. Rev. B **86**, 115427 (2012).
[25] K. S. Virk and J. E. Sipe, Phys. Rev. Lett. **107**, 120403 (2011).
[26] J. Rioux, J. E. Sipe, and G. Burkard, Bulletin of the American Physical Society, APS March Meeting **59**(1), D30.00009 (2014).
[27] See Supplemental Material at http://link.aps.org/supplemental/10.1103/PhysRevB.89.205113 for details of the derivation of the formulas in Sec. II.
[28] Here we are still using a discrete momentum basis; the derivative can be obtained from the extension of the function $H_{\boldsymbol{k}}$ to continuum momenta and then restricting $\partial_{k^a} H_{\boldsymbol{k}}$ back to discrete momentum space.
[29] See Supplemental Material at http://link.aps.org/supplemental/10.1103/PhysRevB.89.205113 for the computation of the optical injection coefficients for a generic two-band system.
[30] C.-X. Liu, X.-L. Qi, H. J. Zhang, X. Dai, Z. Fang, and S.-C. Zhang, Phys. Rev. B **82**, 045122 (2010).
[31] H.-Z. Lu, W.-Y. Shan, W. Yao, Q. Niu, and S.-Q. Shen, Phys. Rev. B **81**, 115407 (2010).
[32] H. Zhao, E. J. Loren, H. M. van Driel, and A. L. Smirl, Phys. Rev. Lett. **96**, 246601 (2006).
[33] E. Ya. Sherman, A. Najmaie, H. M. van Driel, A. L. Smirl, and J. E. Sipe, Solid State Commun. **139**, 439 (2006).
[34] See Supplemental Material at http://link.aps.org/supplemental/10.1103/PhysRevB.89.205113 for the optical injection coefficients for the surfaces of topological insulators.
[35] C. W. Luo, H. J. Wang, S. A. Ku, H.-J. Chen, T. T. Yeh, J.-Y. Lin, K. H. Wu, J. Y. Juang, B. L. Young, T. Kobayashi, C.-M. Cheng, C.-H. Chen, K.-D. Tsuei, R. Sankar, F. C. Chou, K. A. Kokh, O. E. Tereshchenko, E. V. Chulkov, Yu. M. Andreev, and G. D. Gu, Nano Lett. **13**, 5797 (2013).
[36] See Supplemental Material at http://link.aps.org/supplemental/10.1103/PhysRevB.89.205113 for intermediate steps in the computations of formulas shown in the appendixes.